Electron Transfer Kinetics of Aquated $Fe^{+3/+2}$, $Eu^{+3/+2}$, and $V^{+3/+2}$ at Carbon Electrodes

Inner Sphere Catalysis by Surface Oxides

Christie Allred McDermott, Kristin R. Kneten,* and Richard L. McCreery**

Department of Chemistry, The Ohio State University, Columbus, Ohio 43210

ABSTRACT

The electron-transfer kinetics for three aquated metal ions with low self-exchange rates were examined on well-characterized carbon surfaces. All three ions exhibited slow kinetics on clean fractured glassy carbon (GC) and on the basal plane of highly ordered pyrolytic graphite (HOPG). The reactions appeared to be outer sphere and had rates approximately consistent with those predicted from the self-exchange rates. Electrochemical oxidation of either GC or HOPG greatly increased the electron-transfer rate constant to values significantly greater than predicted for outer-sphere reactions. The increase was greatest for $Eu_{aq}^{+3/+2}$ and was eliminated if the surface was silanized. Surface oxides provide sites for inner-sphere catalysis of the aquated ions at carbon, perhaps involving a surface oxide structure similar to the common ligand acetoacetonate.

Due principally to their widespread use in electrosynthesis and electroanalysis, carbon electrodes have been examined extensively, with particular attention to factors affecting electrode kinetics and background currents.[1-3] Most previous studies have been dominated by characteristics of the carbon surface and by pretreatments which alter the structure and reactivity of the carbon electrode. Since carbon has several forms and a rich surface chemistry, the task of relating surface structure and reactivity has been formidable. The results of these efforts have been discussed extensively, with particular attention to issues of surface microstructure, cleanliness, roughness, and oxidation.[1,4-11] In general, previous efforts have dealt with relatively few redox systems, particularly $Fe(CN)_6^{-4/-3}$, ascorbic acid, $Ru(NH_3)_6^{+2/+3}$, and several quinones. Of relevance to the current report are the observation that GC exhibits much higher heterogeneous-electron-transfer rate constants (k°) than the basal plane of HOPG,[4,12,13] and that thermal[6,14] or laser[12,13] activation or ultraclean polishing[5,9] greatly increases k° on GC. In addition, the observed kinetics for $Fe(CN)_6^{-3/-4}$ and similar benchmark systems do not correlate with surface oxidation provided the GC surface is initially clean.[1,15] A variety of arguments support the conclusion that activation of HOPG toward $Fe(CN)_6^{-3/-4}$ is not related to oxides *per se,* but rather to lattice damage accompanying their formation.

When the discussion is broadened to a wider variety of redox systems, the picture becomes somewhat more complex and less thoroughly understood. Seven inorganic redox systems normally regarded as outer-sphere systems exhibited k° values 1 to 5 orders of magnitude lower on HOPG than on activated GC,[16] as expected from the $Fe(CN)_6^{-3/-4}$ results noted earlier. In addition, several quinone systems were very slow on HOPG, perhaps because of the lack of sites for proton transfer.[11] Several workers have noted that the observed k° for $Fe^{+3/+2}$ increases when a polished GC surface is oxidized,[10,17,18] sometimes by factors of more than 100. Kovach *et al.* have reported large effects of electrochemical pretreatment (ECP) on the behavior of several metal complexes as well as dopamine and ascorbate, due largely to discrimination of the oxidized surface for cations over anions.[19] Armstrong *et al.* have described the importance of oxide sites to cytochrome charge transfer on carbon, with binding of the cytochrome to a surface oxide greatly accelerating electron transfer.[20,21] Cabaniss *et al.*,[11] Kepley and Bard,[22] and Nagaoka *et al.*[23,24] also have attributed kinetic activation of electrochemically pretreated GC to surface oxides. These results imply that different redox systems are affected differently by carbon surface variables, with some dependent on surface oxides and others not.

The issue of relating carbon surface structure to electron-transfer reactivity is important to the broader area of electrode kinetics. A large research effort has been invested in understanding the relationship between k° and homogeneous-electron-transfer rates, particularly in the context of Marcus theory.[25-34] To simplify the problem as much as possible, attempted correlations of k° and homogeneous rates used well-defined electrodes, particularly mercury. For outer-sphere redox systems after suitable work-term and double-layer corrections, k° tracks the square root of the homogeneous-self-exchange rate constant (k_{exc}) as predicted by Marcush theory.[31,34] The existence of an inner-sphere reaction pathway (such as a halide-bridging ligand on a platinum electrode) can greatly increase k° over that predicted from k_{exc}.[35-37] While significant progress has been made toward understanding and predicting k° on well-defined metal electrodes, such progress for carbon electrodes has been frustrated by their complex surface. The long-term goal of our work in this area is to understand both electrode-surface and redox-system variables which control k° on carbon.

Although polished GC is the most widely studied GC surface, its oxide coverage is variable, typically 7 to 15 atom percent (a/o),[1] and the involvement of oxide catalyzed routes in electron transfer is difficult to assess. Our approach here is to start with better defined carbon surfaces with very low oxide coverage. Basal plane HOPG is one example of a well-defined carbon surface with near zero surface oxides, provided it is prepared properly. We have reported also that the freshly exposed surface of GC is quite reactive for several redox systems.[12] Although it is rougher than polished GC,[38,39] it is initially free of oxides or polishing debris, and should closely approximate a pristine GC surface. The current report concerns the behavior of aquated $Fe^{+3/+2}$, $Eu^{+3/+2}$, and $V^{+3/+2}$ on HOPG and fractured GC before and after electrochemical oxidation of the carbon surface. In addition to the fact that HOPG and fractured GC provide less complex and better defined carbon surfaces than more conventional electrodes, the aquated redox systems exhibit unusual kinetic behavior which permits useful conclusions about electron-transfer mechanisms at carbon electrodes. The primary advantage of the current approach is the low initial surface oxide concentration on HOPG and fractured GC.

Experimental

Electrode preparation.—Glassy carbon (GC-20) electrodes were prepared from GC-20 plate as described previously.[12,39] Polished GC electrodes were prepared by initial sanding of the epoxy (Eccobond) mounted GC with SiC

* Electrochemical Society Student Member.
** Electrochemical Society Active Member.

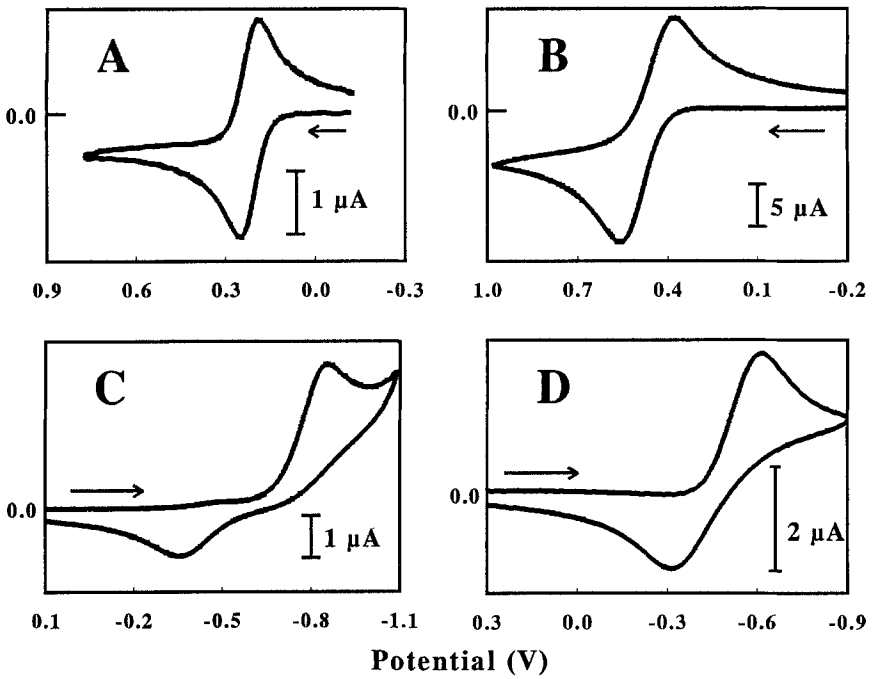

Fig. 1. Voltammetry at fractured GC; (A) 1 mM $Fe(CN)_6^{3-/4-}$ in 1M KCl, ΔE_p = 58 mV; (B) 5 mM $Fe^{2+/3+}$ in 0.2M $HClO_4$, ΔE_p = 181 mV; (C) 5 mM $Eu^{3+/2+}$ in 0.2M $HClO_4$, ΔE_p = 503 mV; and (D) 3 mM $V^{3+/2+}$ in 0.2M $HClO_4$, ΔE_p = 304 mV; ν = 0.2 V/s, voltammograms were all background-subtracted. Arrows indicate initial scan direction.

grinding paper, then polishing with successive 1, 0.3, and 0.05 μm alumina slurries on Microcloth polishing cloth (Buehler). Polished electrodes were sonicated in NANOpure water (Barnstead) for approximately 5 min before placement in the electrochemical cell. During transfer, exposure of the electrode surface to air was reduced by keeping the surface wet. Fractured surfaces were created by first filing away the embedding epoxy and exposing a short length of GC post. The fractured surface was created *in situ* by breaking this postflush with the epoxy surface.[40] The exposed GC surface remaining embedded in the epoxy served as the electrode surface. For both polished and fractured electrodes the exposed GC surface area was 0.003 to 0.008 cm^2. Voltammetry was performed immediately (within 5 s) of fracturing.

Laser activation of HOPG and polished GC electrodes was performed with a Nd:YAG laser (Quantel) operating at 1064 nm with 9 ns pulses.[12,13] To average spatial variations of the laser, three successive pulses were applied to the electrode. Power densities were 25 MW/cm^2 for GC surfaces and 50 MW/cm^2 for HOPG surfaces. For both HOPG and GC, laser activation was performed in 1M H_2SO_4. Electrochemical pretreatment procedures were all performed by cycling from 0 to 2.2 V *vs.* Ag/AgCl at 0.2 V/s. For HOPG electrodes, this procedure was performed in 0.1M H_2SO_4 for 20 cycles. For GC electrodes, this procedure was performed in 1M H_2SO_4 for 1 to 13 cycles, as discussed later. Generally, 1 to 5 cycles were necessary to observe full activation on GC.

HOPG was obtained from Arthur Moore at Union Carbide and was cleaved with adhesive tape before use. Since laser activation and ECP required an electrochemical cell, the inverted drop cell and validation procedure reported previously[16,41] were not employed. The term validation is used here to refer to HOPG basal plane surfaces which were verified to have high ΔE_p for $Fe(CN)_6^{-3/-4}$ (ΔE_p > 700 mV) as an indication of low defect density.[16]

The procedure for surface modification with organosilanes was similar to literature techniques.[20,21,42] A fractured GC surface was electrochemically pretreated with one cycle under the conditions stated above. The electrode was rinsed and a Kimwipe used to wick off residual water before placing the electrode in neat chlorotrimethylsilane for 5 h. The chlorotrimethylsilane liquid was kept under argon before and during the derivatization procedure. Upon removal from the chlorotrimethylsilane, the electrode was washed once or twice with methanol for 30 min. Voltammetry was performed after the first and second methanol washes. The electrode then was placed in saturated KOH/methanol solution for 1 h to remove the silane, after which final voltammetric measurements were performed. To ensure that the changes in the observed voltammetry were due to derivatization of surface oxides, a control experiment was performed in which tetramethylsilane was used instead of chlorotrimethylsilane but otherwise identical conditions were employed. The tetramethylsilane is not labile toward substitution, and surface oxides are unaffected.

Electrochemical measurements.—Cyclic voltammetry was performed at 0.2 V/s as described previously,[38] with an analog triangular waveform and a laboratory computer. For GC and HOPG experiments, the electrochemical cell was constructed of Teflon and was equipped with a quartz window through which the electrode could be laser irradiated. The three-electrode cell was completed with a Bioanalytical Systems Ag/AgCl (3M NaCl) reference electrode and a platinum wire auxiliary electrode. Electrode areas for HOPG were defined by an o-ring and were approximately 0.02 cm^2.

Rate constants for GC were calculated by the method of Nicholson,[43] assuming α = 0.5; k° values for HOPG were obtained through comparison of experimental voltammetry to simulations involving a potential-dependent α.[44] The rate constants were calculated with literature values for diffusion coefficients: Fe^{2+}_{aq}, $D_R = 9 \times 10^{-6}$ cm^2/s (0.1M $HClO_4$);[45,46] Eu^{+3}_{aq}, $D_o = 7.9 \times 10^{-6}$ cm^2/s (pH 0.3, 1M $NaClO_4$/$HClO_4$);[47] V^{+3}_{aq}, $D_o = 5.2 \times 10^{-6}$ cm^2/s (1M $HClO_4$).[48] In all cases, it was assumed that $D_R = D_o$ for the rate-constant calculations.

Reagents.—Fe^{2+}_{aq} and Eu^{+3}_{aq} solutions were prepared at 5 mM concentrations for GC experiments and at 10 mM concentrations for HOPG experiments from $Fe(NH_4)_2(SO_4)_2 \cdot 6H_2O$ (J.T. Baker, Inc.) and $Eu(NO_3)_3 \cdot (H_2O)_5$ (Aldrich). V^{3+}_{aq} solutions were prepared at 3 to 5 mM concentrations for GC and HOPG experiments from VCl_3 (Aldrich). Supporting electrolyte solutions were prepared with 70% $HClO_4$ (GFS Chemicals) at a concentration of 0.2M unless specified otherwise. $HClO_4$ was used as the supporting electrolyte due to its weak interaction with aquated metal ions.[37,49,50] Electrochemical pretreatment and laser activation procedures were performed in H_2SO_4 (Mallinckrodt). All solutions were prepared with NANOpure water and were degassed with argon or nitrogen prior to use. $ClSiMe_3$ and $SiMe_4$ were obtained from Aldrich, and $ClSiMe_3$ was distilled before use.

Table I. ΔE_p (mV) values at GC and HOPG electrodes under different pretreatment conditions.[a]

	Polished GC	Polished GC/ laser activated (3 × at 25 MW/cm²)[b]	Fractured GC	Frac/ECP[c] GC	HOPG	HOPG/ECP[d]
$Fe_{aq}^{+3/+2}$	258 ± 39[e] [5][f]	263 [2]	186 ± 19 [9]	93 ± 11 [6]	1062 ± 225 [9]	162 ± 22 [4]
$Eu_{aq}^{+3/+2}$	428 ± 27 [7]	>531 [3]	509 ± 42 [8]	70 ± 4 [4]	936 ± 168 [5]	193 ± 18 [3]
$V_{aq}^{+3/+2}$	441 ± 72 [6]		314 ± 13 [4]	95 ± 9 [4]	>835 [4]	372 ± 6 [3]

[a] ν = 0.2 V/s.
[b] Laser activation performed in 1.0*M* H_2SO_4.
[c] ECP procedure for GC consisted of cycling from 0 to 2.2 V at 0.2 V/s for 3 to 5 cycles.
[d] ECP procedure same as GC, but 20 cycles.
[e] Standard deviation.
[f] Number of trials.

Results

The first issue to consider is the kinetic behavior of $Fe_{aq}^{+3/+2}$, $Eu_{aq}^{+3/+2}$, and $V_{aq}^{+3/+2}$ on carbon surfaces which are as well characterized as currently possible. When considering the voltammograms of Fig. 1 to 3, a visual indication of increased electron-transfer rate is a decrease in ΔE_p, which is then reflected in the k° results. Figure 1 shows voltammograms for the aquated systems and $Fe(CN)_6^{-3/-4}$ on a GC surface immediately after exposure to the solution by fracturing. It is clear that the aquated ions are kinetically slower than $Fe(CN)_6^{-3/-4}$ on fractured GC. As indicated in Table I, laser activation of a polished GC surface has little effect on $Fe_{aq}^{+3/+2}$ and $Eu_{aq}^{+3/+2}$ kinetics, in contrast to the large increase in rate observed for $Fe(CN)_6^{-3/-4}$.[1,13] Figure 2 shows voltammograms obtained on HOPG, with all four redox systems exhibiting much larger ΔE_p values than on GC. Although the use of a conventional cell prevented validation of the HOPG surfaces,[16] the ΔE_p values listed in Table I were reproducibly high, exceeding 800 mV for the aquated ions. Thus the behavior of $Fe_{aq}^{+3/+2}$, $Eu_{aq}^{+2/+3}$, and $V_{aq}^{+3/+2}$ on either fractured GC or basal plane HOPG is consistent with slow electron-transfer kinetics.

Figure 3A and B shows the dramatic effect of one ECP cycle on the voltammetry of $Fe^{+3/+2}$ and $Eu^{+3/+2}$ on GC. After even this minimal treatment, ΔE_p for $Eu^{+3/+2}$ decreased from 440 mV for the fractured surface to 76 mV (Table I). $Fe^{+3/+2}$ and $V^{+3/+2}$ also exhibited major decreases in ΔE_p on ECP. Figure 4 shows the effects of successive ECP cycles on ΔE_p, with the greatest changes occurring in the first few cycles. A qualitatively similar effect was observed for HOPG, although a larger number of ECP cycles was required (20 *vs.* 1 to 3). The voltammetry for $Fe^{+3/+2}$ and $Eu^{+3/+2}$ on HOPG before and after ECP is shown in Fig. 3C and D, and the results are listed in Table I.

To test whether the kinetic effects of ECP are mediated by surface oxides, the surface was silanized with $ClSiMe_3$. The unreactive $SiMe_4$ acted as a control. The effects of silanization on $Eu^{+3/+2}$ voltammetry are shown in Table II, with entries A to E representing successive treatments, starting with fractured GC. $ClSiMe_3$ completely negates the effects of ECP-induced activation on $Eu^{+3/+2}$ kinetics (entry C), while hydrolysis of the silanized surface with base restores most of the reactivity of the ECP surface (entry E). The $SiMe_4$ reagent increases ΔE_p somewhat, but its effects are much smaller and probably due to adsorption of organic impurities. Table II demonstrates that the ECP-induced activation of $Eu^{+2/+3}$ charge transfer on GC is eliminated by silanization.

The possibility of Cl^- catalysis[35-37] on GC was tested by adding small amounts of Cl^- to the electrolyte. For Au and Pt electrodes, Cl^- chemisorption greatly accelerates $Fe^{+2/+3}$ electron transfer even at low ($10^{-5}M$) Cl^- concentrations. Neither 10^{-4} nor 0.2*M* Cl^- had any observable effect on $Fe^{+2/+3}$ voltammetry at fractured GC. High (1*M*) Cl^- did increase k° for $Eu^{+3/+2}$ on fractured GC, probably via formation of a chloro complex of $Eu^{+3/+2}$ rather than a bridging

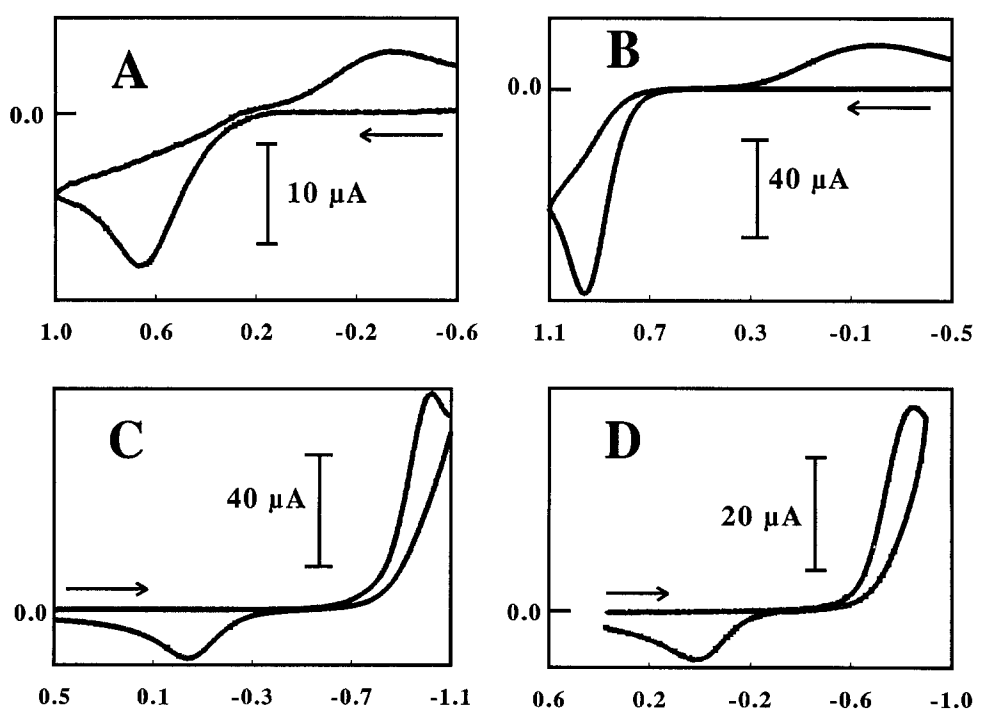

Fig. 2. Voltammetry at HOPG; (A) 1 mM $Fe(CN)_6^{3-/4-}$ in 1*M* KCl, ΔE_p = 1007 mV; (B) 10 mM $Fe^{2+/3+}$ in 0.2*M* $HClO_4$, ΔE_p = 1164 mV; (C) 10 mM $Eu^{3+/2+}$ in 0.2*M* $HClO_4$, ΔE_p = 980 mV; (D) 5 mM V^{+3} in 0.2*M* $HClO_4$, ΔE_p = 860 mV; ν = 0.2 V/s, voltammograms were not background-subtracted; $Fe(CN)_6^{3-/4-}$ voltammetry was obtained using an inverted drop cell as described in Ref. 16. All others were obtained in a cell as described in the Experimental section.

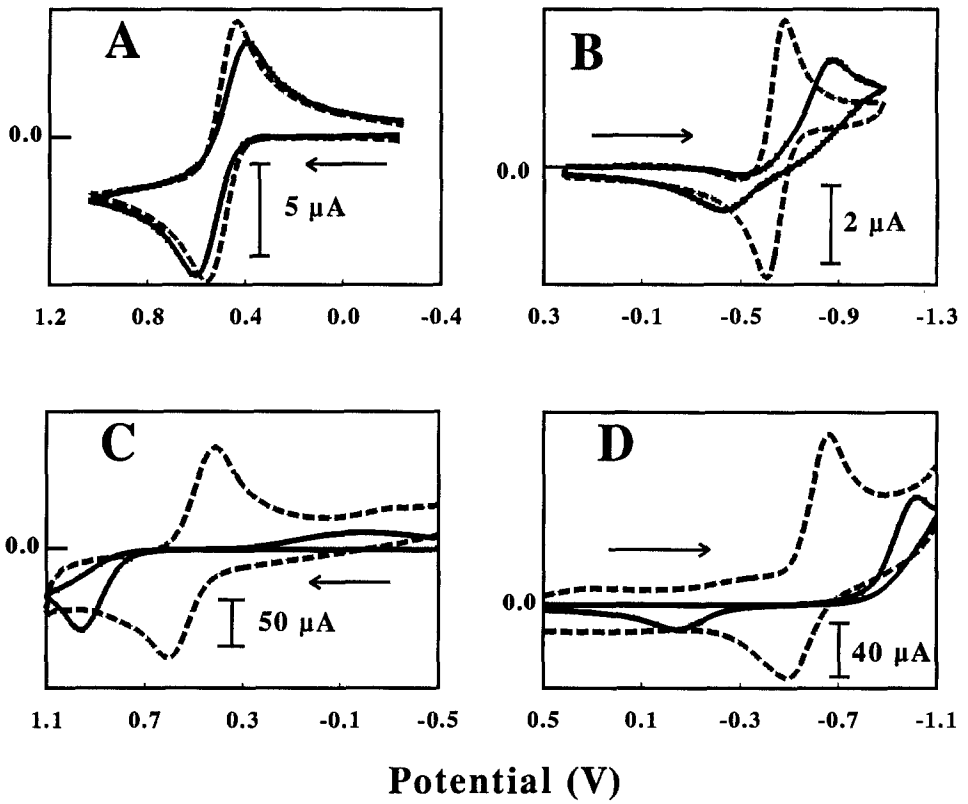

Fig. 3. Voltammetry of Fe^{+2} and Eu^{+3} at HOPG and fractured GC electrodes (solid curves) and the same surfaces after ECP (dashed curves); (A) 5 m*M* Fe^{+2} on fractured GC and fractured/ECP GC; (B) 5 m*M* Eu^{+3} on fractured GC and fractured/ECP GC; (C) 10 m*M* Fe^{+2} on HOPG and HOPG/ECP; and (D) 10 m*M* Eu^{+3} on HOPG and HOPG/ECP; ν = 0.2 V/s, voltammograms on GC were background subtracted, ECP procedure on GC was 1 cycle from 0 to 2.2 V in 1*M* H_2SO_4, ECP procedure on HOPG was 20 cycles from 0 to 2.2 V in 0.1*M* H_2SO_4.

mechanism. Finally, the possibility that freshly fractured GC was oxidized by dissolved oxygen was tested by repeating the kinetic measurement in 1*M* $HClO_4$ saturated with air. No change in the behavior of $Fe^{+2/+3}$ was observed, neither initially nor after 1 h in air-saturated electrolyte.

Discussion

Past efforts to characterize carbon electrode surfaces have led to the proposal that fractured GC is the GC surface least modified by impurities, oxides, and intentional surface chemical changes.[12,38-40] Accordingly, the fractured GC surface should represent the closest approximation currently available to a pristine GC surface. Similarly, low-defect HOPG basal plane is an ordered surface of known structure which has been characterized electrochemically. These two electrode materials provide good reference surfaces for evaluating the kinetics of various redox systems on carbon electrodes. We reported previously the heterogeneous rate constants for several redox systems on HOPG and laser-activated GC.[16] Although the rate constants on HOPG were significantly lower than those on GC, they did correlate with homogeneous-self-exchange rate constants (k_{exc}). Unfortunately, the k° values on laser-activated or fractured GC are near or above the upper instrumental limit for the systems studied previously, so reliable correlations of k° and k_{exc} were not possible for GC.

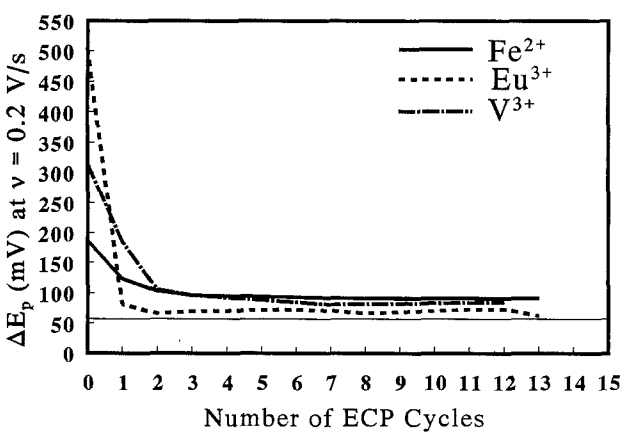

Fig. 4. Decrease in peak separation with number of ECP cycles for Fe^{2+}_{aq}, Eu^{3+}_{aq}, and V^{3+}_{aq} on fractured GC. ECP procedures employed 0 to 2.2 V cycles in 1*M* H_2SO_4. Line indicates reversible limit.

First for the unoxidized carbon surfaces, it is possible to relate k° to k_{exc} for $Fe^{+3/+2}_{aq}$, $Eu^{+3/+2}_{aq}$, and $V^{+3/+2}_{aq}$, in part because their k° values are well within the measurable range. The first four columns of Table III compare kinetic data and predictions for five redox systems on fractured GC and basal-plane HOPG. The theoretical k° values, (k°_{th}) were calculated from the simplest Marcus equation

$$\left(\frac{k_{exc}}{Z_{exc}}\right)^{1/2} = \frac{k^\circ}{Z_{el}} \qquad [1]$$

where $Z_{exc} = 10^{11}\ M^{-1}\ s^{-1}$ and $Z_{el} = 10^4\ cm\ s^{-1}$. Several important work-term and double-layer corrections have been developed for this expression by Weaver *et al.*, but both the simple and corrected expression predict that k° tracks $k^{1/2}_{exc}$.[31-34] Since these corrections are not yet possible for carbon electrodes due to their unknown double-layer properties, we shall use Eq. 1 as a first approximation for predictions of k°_{th} from k_{exc}.

Several observations are available from Table III. First, the five redox systems cover a wide range of predicted k°_{th}, with the aquated ions easily within the measurable range of rate constants. Second, the k° on fractured GC (k°_{frac}) is within a factor of 16 of that predicted from Eq. 1. Third,

Table II. Effects of silanization on $Eu^{+3/+2}_{aq}$ voltammetry.

	ΔE_p (mV)[a] Reagents	
	$ClSiMe_3$	$SiMe_4$
A. Fractured GC	490	492
B. Fractured after ECP	70	68
C. B. + silane + MeOH wash	442	149
D. C. + second MeOH wash	470	202
E. D. + KOH/MeOH wash	123	110

[a] ΔE_p values were acquired at 0.2 V/s and are averages of two trials for both reagents.

Table III. Kinetic results for fractured GC and HOPG.

System	k_{exc} (M^{-1} s^{-1})	k°_{th} [b] (cm/s)	k°_{frac} [c] (cm/s)	k°_{HOPG} [d] (cm/s)	$k^{\circ}_{ECP/GC}$ (cm/s)
$Fe^{+3/+2}_{aq}$ [a]	1×10^{-3}	1×10^{-3}	$(2.3 \pm 0.5) \times 10^{-3}$ [8]	1.4×10^{-5} [3]	$(1.2 \pm 0.3) \times 10^{-2}$ [5]
$Eu^{+3/+2}_{aq}$ [a]	2×10^{-4}	4×10^{-4}	$(8 \pm 4) \times 10^{-5}$ [8]	2.5×10^{-6} [2]	$(4.0 \pm 0.1) \times 10^{-2}$ [4]
$V^{+3/+2}_{aq}$ [a]	0.05	7×10^{-3}	$(4.5 \pm 0.5) \times 10^{-4}$ [4]	$<3 \times 10^{-6}$ [1]	$(8.7 \pm 0.3) \times 10^{-3}$ [4]
$Fe(CN)^{-3/-4}_{6}$ [e]	2×10^{4}	4.2	≥ 0.5	$<10^{-6}$	
$Ru(NH_3)^{+2/+3}_{6}$ [e]	4×10^{3}	1.9	0.3	9×10^{-4}	

[a] k_{exc} data from Ref. 34.
[b] Calculated from Eq. 1.
[c] Rate constants indicate mean and standard deviation, number in brackets is number of trials.
[d] HOPG rate constants obtained from comparison to simulations for HOPG C-V's; surfaces were not validated.
[e] Data from Ref. 16.

k°_{frac} is lower than k°_{th} for all cases except $Fe^{+3/+2}$, consistent with Hupp and Weaver's observations of the effects of work terms on k° for mercury electrodes.[34] Fourth, k° on HOPG is much lower than both k° on fractured GC and k°_{th} as observed previously for numerous outer-sphere systems.[16] The most likely cause of this difference is the low density of electronic states in HOPG. As noted in the Experimental section, the HOPG surfaces were not validated due to the use of a cell rather than inverted drop (resulting in strain-induced defects), so the k°_{HOPG} values represent upper limits of the true basal-plane values. Fifth, a least squares line for a plot of log k°_{frac} *vs.* log k_{exc} for the systems in Table III has a slope of 0.42 ± 0.08, intercept of -2.2 ± 0.6, and a correlation coefficient of 0.95. Although the fit is not as good as that for a more sophisticated treatment of the aquated redox systems on a mercury electrode,[34] the slope and intercept are near the values of 0.50 and -1.5 predicted from Eq. 1. Since the double-layer and work-term corrections for carbon electrodes are not available, the observed heterogeneous rate constants observed on fractured GC are approximately consistent with Eq. 1. Finally, the rates on fractured GC were slightly higher than those on laser-activated GC for the aquated ions (see Table I), but this difference is insignificant compared to the difference between GC and HOPG.

The overall conclusion for fractured GC and HOPG before ECP is that $Fe^{+3/+2}$, $Eu^{+3/+2}$, and $V^{+3/+2}$ behave approximately the same as outer-sphere systems such as $Ru(NH_3)^{+3/+2}_{6}$, $IrCl^{-2/-3}_{6}$, etc. In particular, the observed k° for fractured GC (when it can be measured) is within an order of magnitude of that predicted from Eq. 1, and the deviation from k°_{th} is generally on the low side. As was the case for previous outer-sphere systems, aquated ions exhibit substantially slower kinetics on HOPG, probably because of the unusual electronic properties of HOPG. Figure 5 shows the aquated ion results from fractured GC and HOPG plotted together with previous data for other redox systems. Although the scatter is significant, the aquated ions follow the same trends as the faster outer-sphere systems.

Although the kinetics observed on fractured GC and HOPG for the aquated ions are reasonably consistent with that expected for outer-sphere electron transfer, the behavior following electrochemical surface oxidation is different. As shown in Fig. 3 and Table III (fifth column), ECP significantly increases k°, by factors of 5.2 (for $Fe^{+3/+2}$), 19 ($V^{+3/+2}$), and 500 ($Eu^{+3/+2}$). For $Eu^{+2/+3}$, the ECP-induced rate increase is eliminated reversibly by silanization, indicating that the rate enhancement is mediated by surface oxides. The intent of using HOPG basal plane and fractured GC was to compare ECP surfaces with reference surfaces as low as possible in surface oxides. Low defect HOPG is certainly low in oxides, and fractured GC also has zero oxide coverage, at least at the instant of fracture. Schrader[51,52] used x-ray photoemission spectroscopy (XPS) to demonstrate that argon-ion-damaged HOPG does not react with H_2O to form surface oxides in UHV conditions. That saturation of the solution with air before fracturing has no effect on the $Fe^{+2/+3}$ rate implies that oxidation by air does not lead to a catalytically active surface. It is difficult to rule out low levels of oxides on fractured GC, but it is clear that ECP causes a major rate increase, and that fractured GC is a useful reference surface exhibiting primarily outer-sphere electron transfer. Thus the kinetic behavior exhibited in Fig. 1 and 2 and the third and fourth columns of Table III is that for surfaces with minimal (if any) oxide related catalysis.

The possible origins of the ECP-induced rate may involve several phenomena, including indirect effects such as double-layer corrections, changes in hydrophobicity or adsorption, or more direct effects such as inner-sphere catalysis. While ECP-induced oxide formation may alter double-layer structure substantially, such effects seem unlikely in the aquated ions studied here. A double-layer correction should depend strongly on the position of $E_{1/2}$ relative to the pzc (-0.2 *vs.* Ag/AgCl for HOPG,[53,54] *ca.* +0.1 V for GC).[55] Yet all three systems show rate increases even though they have $E_{1/2}$ values ranging from *ca.* +0.5 to -0.7 V *vs.* Ag/AgCl. Wightman *et al.* showed that Frumkin effects are observed for GC at elevated pH where surface carboxylates are deprotonated, but disappeared below pH 3.[56] All the current results were obtained in 0.2*M* acid, where carboxylates should be uncharged. Adsorption to the oxidized surface was tested by comparing experimental and simulated voltammograms and by semi-integration.[57] No evidence of adsorption was observed on the surfaces formed by 3 to 5 ECP cycles, although some was apparent for heav-

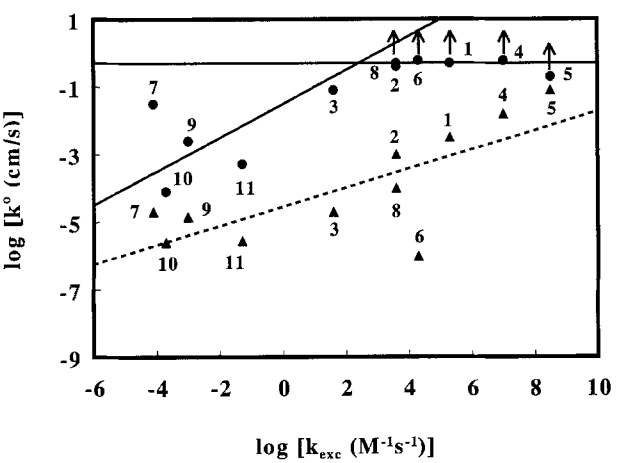

Fig. 5. Log-log plot for heterogeneous rate constants (k°) *vs.* homogeneous self-exchange rates (k_{exc}) for redox systems in Table III and from Ref. 16, Table II. Triangles are for HOPG basal plane, circles are for GC. Solid line is from Marcus theory, Eq. 1 in text. Dashed line is least squares fit for all points, HOPG data: slope = 0.28, y-intercept = −4.5, correlation coefficient = 0.75. Horizontal line indicates upper limit of measurable rate constants for GC experiments, k° = 0.5 cm/s. Number assignments for redox systems are: (1) $IrCl^{-2/-3}_{6}$; (2) $Ru(NH_3)^{+3/+2}_{6}$; (3) $Co(phen)^{+3/+2}_{3}$; (4) $MV^{+2/+1}$; (5) $Fe(phen)^{+3/+2}_{3}$; (6) $Fe(CN)^{-3/-4}_{6}$; (7) $Co(en)^{+3/+2}_{3}$; (8) $Ru(en)^{+3/+2}_{3}$; (9) $Fe^{+3/+2}_{aq}$; (10) $Eu^{+3/+2}_{aq}$; and (11) $V^{+3/+2}_{aq}$.

ily oxidized surfaces. The oxidized surface is probably less hydrophobic than fractured GC and certainly less than HOPG, but hydrophobic effects did not appear important for the series of outer-sphere systems studied previously. Redox systems of different electrostatic charge, and presumably different sensitivity to hydrophobic effects, did not vary greatly in rate on HOPG.[16]

The key observation leading to the origin of the ECP-induced rate increase is that ECP yields k° values above those predicted by Eq. 1 for outer-sphere electron transfer. Furthermore, inner-sphere catalysis via bridging groups has been reported for $Fe^{+2/+3}$ on Pt and Au in Cl^- media,[35-37] and for $Fe^{+2/+3}$ in cytochromes on polished graphite.[21] In the latter case, catalysis was blocked by silanization or cationic species such as Mg^{+2}. The observations lead to a proposal that surface oxides on carbon provide an inner-sphere route for electron transfer to $Fe_{aq}^{+3/+2}$, $Eu_{aq}^{+3/+2}$, and $V_{aq}^{+3/+2}$ which increases the rate constant substantially over the outer-sphere value. Oxide catalysis at GC is analogous to Cl^- catalysis of $Fe^{+3/+2}$ at Au and Pt, and likely involves a qualitatively similar bridging mechanism. ECP also reduced the rate differences among the three aquated ions observed on the fractured GC surface, with the k°_{frac} values differing by a factor of 28 and $k^\circ_{GC/ECP}$ by a factor of 5. For a bridging mechanism to be significant for $Fe_{aq}^{+2/+3}$, $Eu_{aq}^{+2/+3}$, and $V_{aq}^{+2/+3}$, the aquated ions must be substitution labile. The water-exchange rate constants for several relevant ions are as follows, all expressed as common logorithms: Fe^{+2}, 6.64; Fe^{+3}, 2.20; V^{+2}, 1.9; V^{+3}, 2.7;[58] and Ru^{+2}, −1.84; Ru^{+3}, −5.3.[59] $Eu^{+2/+3}$ water exchange is too fast to measure, but similar lanthanides have water-exchange rate constants in the range of 10^7 to 10^9 M^{-1} s^{-1}.[60] Thus $Fe_{aq}^{+2/+3}$, $Eu_{aq}^{+2/+3}$, and $V_{aq}^{+2/+3}$ exhibit fast ligand exchange rates compared to the substitution inert $Ru^{+2/+3}$ systems.

The inhibition of oxide catalysis by silanization implies the involvement of -OH, -COOH, or similar hydroxyl-containing functional groups in the inner-sphere route. Although hydroxyl-containing functional groups in the inner-sphere route. Although hydroxyl and carboxylate functional groups have long been known to occur on oxidized carbon surfaces, a structure proposed by Kozlowski and Sherwood[61] may be particularly relevant here. XPS spectra of carbon fibers after ECP supports the formation of structure 1. This structure may exist primarily as structure 2, which is itself similar to the common inorganic ligand acetoacetonate (acac). Presumably the formation of structure 2 would be prevented by silanization.

Structures

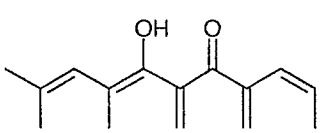

(1)

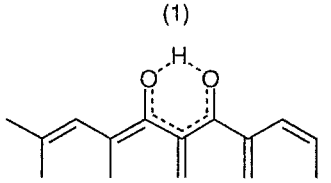

(2)

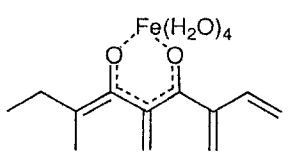

(3)

The aquated ions studied here are fairly weak and substitution labile, while the corresponding acac complexes are quite strong (*e.g.*, K_{form} for $[Fe(III)acac(H_2O)_4]^{+2}$ is 10^{10}).[62] It is reasonable to propose that inner-sphere catalysis of $Fe_{aq}^{+3/+2}$, $Eu_{aq}^{+3/+2}$, and $V_{aq}^{+3/+2}$ involves an intermediate such as structure 3. The relatively strong interaction of the metal ion with the surface acac group may provide the driving force for inner-sphere catalysis, and possibly for displacement of the proton in structure 2.

In summary, the $Fe_{aq}^{+3/+2}$, $Eu_{aq}^{+3/+2}$, and $V_{aq}^{+3/+2}$ redox systems are slow on either fractured GC or HOPG, as is consistent with their low self-exchange rates. On fractured GC with presumably low oxide coverage, the observed rate constants are approximately those predicted from simple Marcus theory. Even minor electrochemical oxidation of the GC (or HOPG) surface leads to large increases in observed rate constants, consistent with an oxide mediated inner-sphere catalytic route. A surface oxide structure observed on oxidized carbon fibers is a possible site for transient metal-ion binding and catalysis, although alternative mechanisms based on double-layer or hydrophobic effects cannot be ruled out completely.

Acknowledgment

This work was supported by a grant from the Air Force Office of Scientific Research and an ACS Analytical Division Fellowship sponsored by Eli Lilly for CAM. The authors thank John Pudelski for assistance with the silanization procedure.

Manuscript submitted Feb. 11, 1993; revised manuscript received June 4, 1993.

The Ohio State University assisted in meeting the publication costs of this article.

REFERENCES

1. R. L. McCreery, in *Electroanalytical Chemistry,* Vol. 17, A. J. Bard, Editor, Dekker, New York (1991).
2. K. Kinoshita, *Carbon: Electrochemical and Physicochemical Properties,* Wiley, New York (1988).
3. S. Sarangapani, J. R. Akridge, and B. Schumm, Editors, *Proceedings of the Workshop on the Electrochemistry of Carbon,* The Electrochemical Society, Pennington, NJ (1984).
4. R. M. Wightman, M. R. Deakin, P. M. Kovach, P. M. Kuhr, and K. J. Stutts, *This Journal,* **131,** 1578 (1984).
5. I. F. Hu, D. H. Karweik, and T. Kuwana, *J. Electroanal. Chem.,* **188,** 59 (1985).
6. D. T. Fagan, I. F. Hu, and T. Kuwana, *Anal. Chem.*, **57,** 2759 (1985).
7. M. R. Deakin, P. M. Kovach, K. J. Stutts, and R. M. Wightman, *ibid.*, **58,** 1474 (1986).
8. G. N. Kamau, W. S. Willis, and J. F. Rusling, *ibid.*, **57,** 545 (1985).
9. D. C. Thornton, K. T. Corby, V. A. Spendel, J. Jordan, A. Robbat, D. J. Rutstrom, M. Gross, and G. Ritzler, *ibid.*, **57,** 150 (1985).
10. R. C. Engstrom and V. A. Strasser, *ibid.*, **56,** 136 (1984).
11. G. E. Cabaniss, A. A. Diamantis, W. R. Murphy, Jr., R. W. Linton, and T. J. Meyer, *J. Am. Chem. Soc.,* **107,** 1845 (1985).
12. R. J. Rice, N. Pontikos, and R. L. McCreery, *ibid.,* **112,** 4617 (1990).
13. M. Poon and R. L. McCreey, *Anal. Chem.,* **58,** 2745 (1986).
14. K. J. Stutts, P. M. Kovach, W. G. Kuhr, and R. M. Wightman, *ibid.,* **55,** 1632 (1983).
15. R. Bowling, R. T. Packard, and R. L. McCreery, *Langmuir,* **5,** 683 (1989).
16. K. R. Kneten and R. L. McCreery, *Anal. Chem.,* **64,** 2518 (1992).
17. R. J. Taylor and A. A. Humffray, *J. Electroanal. Chem.,* **42,** 347 (1973).
18. C. Barbero, J. J. Silber, and L. Sereno, *ibid.,* **248,** 321 (1988).
19. P. M. Kovach, M. R. Deakin, and R. M. Wightman, *J. Phys. Chem.,* **90,** 4612 (1986).
20. F. A. Armstrong and K. J. Brown, *J. Electroanal. Chem.,* **219,** 319 (1987).
21. F. A. Armstrong, A. M. Bond, H. A. O. Hill, B. N. Oliver, and I. S. M. Psalti, *J. Am. Chem. Soc.,* **111,** 9185 (1989).
22. L. J. Kepley and A. J. Bard, *Anal. Chem.,* **60,** 1459 (1988).
23. T. Nagaoka and T. Yoshino, *ibid.,* **58,** 1037 (1986).
24. T. Nagaoka, T. Fukunaga, T. Yoshino, I. Watanabe, T. Nakayama, and S. Okazaki, *ibid.,* **60,** 2766 (1988).
25. R. A. Marcus, *J. Phys. Chem.,* **67,** 853 (1963).

26. J. Kawiak, P. Kulesza, and Z. Galus, *J. Electroanal. Chem.*, **226**, 305 (1987).
27. T. Saji, T. Yamada, and S. Aoyagui, *ibid.*, **61**, 147 (1975).
28. T. Saji, T. Maruyama, and S. Aoyagui, *ibid.*, **86**, 219 (1978).
29. R. Sohr and L. Muller, *Electrochim. Acta*, **20**, 451 (1975).
30. R. Penner, M. Heben, T. Longin, and N. S. Lewis, *Science*, **250**, 1118 (1990).
31. M. J. Weaver and J. J. Zuckerman, Editors, *Inorganic Reactions and Methods*, VCH, **15**, 153-163 (1986).
32. M. J. Weaver, *J. Phys. Chem.*, **84**, 568 (1980).
33. M. J. Weaver, *ibid.*, **15**, 1733 (1976).
34. J. T. Hupp and M. J. Weaver, *Inorg. Chem.*, **22**, 2557 (1983).
35. N. C. Hung and Z. Nagy, *This Journal*, **134**, 2215 (1987).
36. J. Weber, Z. Samec, and V. Marecek, *ibid.*, **89**, 271 (1978).
37. D. C. Johnson and E. W. Resnick, *Anal. Chem.*, **49**, 1918 (1977).
38. N. M. Pontikos and R. L. McCreery, *J. Electroanal. Chem.*, **324**, 229 (1992).
39. M. T. McDermott, C. A. McDermott, and R. L. McCreery, *Anal. Chem.*, **65**, 937 (1993).
40. C. D. Allred and R. L. McCreery, *ibid.*, **64**, 444 (1992).
41. M. T. McDermott, K. Kneten, and R. L. McCreery, *J. Phys. Chem.*, **96**, 3124 (1992).
42. C. M. Elliott and R. W. Murray, *Anal. Chem.*, **48**, 1247 (1976).
43. R. S. Nicholson, *ibid.*, **37**, 1351 (1965).
44. D. A. Corrigan and D. H. Evans, *J. Electroanal. Chem.*, **106**, 287 (1980).
45. R. J. Bowling, Ph.D. Thesis, The Ohio State University, Columbus, OH (1989).
46. M. Stulikova and F. Vydra, *J. Electroanal. Chem. Interfacial Electrochem.*, **38**, 349 (1972).
47. T. Matusinovic and D. E. Smith, *Inorg. Chem.*, **20**, 3121 (1981).
48. J. Lipkowski, A. Czerwinski, E. Ciesznyska, Z. Galus, and J. Sobkoswski, *J. Electroanal. Chem.*, **119**, 261 (1981).
49. M. R. Rosenthal, *J. Chem. Educ.*, **50**, 331 (1973).
50. L. Johansson, *Coord. Chem. Rev.*, **12**, 241 (1974).
51. M. E. Schrader, *J. Phys. Chem.*, **79**, 2508 (1975).
52. M. E. Schrader, *ibid.*, **84**, 2774 (1980).
53. H. J. Gerischer, *ibid.*, **89**, 4249 (1985).
54. H. Gerischer, R. McIntyre, D. Scherson, and W. Storck, *ibid.*, **91**, 1930 (1987).
55. R. K. Jaworski and R. L. McCreery, *This Journal*, **140**, 1360 (1993).
56. M. R. Deakin, K. J. Stutts, and P. M. Wightman, *J. Electroanal. Chem.*, **182**, 113 (1985).
57. R. Bowling and R. L. McCreery, *Anal. Chem.*, **60**, 605 (1988).
58. M. L. Tobe, in *Comprensive Coordinate Chemistry*, Vol. 1, p. 284, G. Wilkinson, Editor, Pergamon Press, New York (1987).
59. P. Bernhard, L. Helm, I. Rapaport, A. Ludi, and A. E. Merbach, *J. Chem. Soc. Chem. Commun.* p. 302 (1984).
60. C. Cossy, L. Helm, and A. E. Merbach, *Inorg. Chem.*, **27**, 1973 (1988).
61. C. Kozlowski and P. M. A. Sherwood, *J. Chem. Soc., Faraday Trans.*, **81**, 2745 (1985).
62. A. E. Martell and R. M. Smith, *Critical Stability Constants*, Vol. 3, pp. 244-247, Plenum Press, New York (1977).

A Quantitative Study of Chemical Etching of InP

Silmara das Neves and Marco.-A De Paoli

Instituto de Química, Universidade Estadual de Campinas, 13081-970 Campinas, SP, Brazil

ABSTRACT

Chemical etching of InP with HCl is used on a large scale, but limited information is available in the literature on the quantitative and mechanistic aspects of this reaction. A higher reaction rate is observed in alcoholic HCl than in aqueous HCl solutions. Also, a decrease of the reaction rate is observed with an increase in the degree of dissociation of HCl in aqueous solutions. We confirm that chemical etching depends on the concentration of nondissociated HCl molecules and that the reaction does not occur below a critical concentration. A first-order rate was obtained in aqueous and in alcoholic HCl solutions. The Arrhenius plot indicated an activation energy greater than 40 kJ · mol^{-1}, indicating a kinetically controlled process. Scanning electron microscopy also showed profiles characteristic of a kinetically controlled process.

There is great interest in the use of indium-phosphorus alloys in optoelectronic devices. During fabrication and quality control of these devices we must use robust and reproducible processes. Chemical etching is used in several steps during the production of such semiconductor devices. Although this technique has been applied since the beginning of this century,[1] it is our opinion that empiricism dominates and etching is still more art than science.

Gerischer *et al.*[2,3] and Notten[4] have shown that the dissolution reaction of semiconductors may occur by a purely chemical mechanism. In such a case, the material surface suffers an attack by reactive solute molecules, as for example halogens and hydrogen halides. These are capable of forming, simultaneously, two new chemical bonds with the semiconductor surface. This concerted action distinguishes such a mechanism from the more usual electrochemical control. The reaction products are dissolved in the etching solution or escape as gases. We view the etching of InP with HCl solutions as an example of this mechanism

$$InP_{(s)} + 3HCl_{(aq)} \rightarrow InCl_{3(aq)} + PH_{3(g)}\uparrow$$

This work was carried out to contribute to the quantitative interpretation of the chemical processes occurring during etching of InP with HCl.

Experimental

The crystals of InP used here were all from single batches of wafers. Samples were doped with Sn and, in some cases, with S. The crystalline orientation of the polished face of the wafers was (001). After cutting small samples from the wafer, the (001) surface was submitted to a mechanochemical polishing with a 2% bromine ethanolic solution at room temperature. Before each etching procedure the samples were extracted with trichloroethylene, acetone, and methanol in a quartz Soxhlet extractor for 10 min and subsequently washed with isopropanol, deionized water, and dried with a high purity nitrogen stream.

To obtain the etching profiles we use a positive photoresist (Shipley S 1400-26) defining 5-μm wide lines by photolithography.

All etching solutions were prepared by dilution of a 12*M* HCl stock solution (standard 37% electronic reagent grade). The etching reactions were performed in a thermostated water bath (5 to 35 ± 0.1°C) in 15 cm^3 glass flasks. The reactions were followed by gravimetry to obtain the reaction rate. The gas produced was qualitatively analyzed using Däger analyzers for phosphine. Scanning electron microscopy (SEM) (Jeol Model JSM-35 CF) was used to observe the etching profiles of the crystals after being cleaved in the orthogonal directions [110] and [$\bar{1}$10].